PAH sampling and quantification from woody biomass fast pyrolysis in a pyroprobe reactor with a modified tar sampling system

Tsekos, C.; Anastasakis, K.; Schoenmakers, P.L.; de Jong, W.

DOI
10.1016/j.jaap.2020.104802

Publication date
2020

Document Version
Final published version

Published in
Journal of Analytical and Applied Pyrolysis

Citation (APA)
Tsekos, C., Anastasakis, K., Schoenmakers, P. L., & de Jong, W. (2020). PAH sampling and quantification from woody biomass fast pyrolysis in a pyroprobe reactor with a modified tar sampling system. *Journal of Analytical and Applied Pyrolysis*, *147*, Article 104802. https://doi.org/10.1016/j.jaap.2020.104802

Journal of Analytical and Applied Pyrolysis 147 (2020) 104802

Contents lists available at ScienceDirect

Journal of Analytical and Applied Pyrolysis

journal homepage: www.elsevier.com/locate/jaap

PAH sampling and quantification from woody biomass fast pyrolysis in a pyroprobe reactor with a modified tar sampling system

C. Tsekos[a,*], K. Anastasakis[a,b], P.L. Schoenmakers[a], W. de Jong[a,c]

[a] Faculty of Mechanical, Maritime and Materials Engineering, Process and Energy Department, Delft University of Technology, Leeghwaterstraat 39, Delft, 2628 CB, The Netherlands
[b] Biological and Chemical Engineering, Department of Engineering, Aarhus University, Hangøvej 2, 8200, Aarhus N, Denmark
[c] Faculty of Science and Engineering Chemical Technology, Engineering and Technology Institute of Groningen, Nijenborgh 4, 9747 AG Groningen, The Netherlands

ARTICLE INFO

Keywords:
Fast pyrolysis
Pyroprobe
Polycyclic aromatic hydrocarbons
Tar
Wood

ABSTRACT

The present work focuses on the sampling procedure and quantification of the PAH yield from the fast pyrolysis of waste softwood. In particular, fast pyrolysis experiments were conducted using a CDS Pyroprobe 5200 at temperatures between 500 °C and 1000 °C, at a heating rate of 600 °C/s for a sample size of 30 mg. High performance liquid chromatography (HPLC) was used for the determination of the PAH compounds present in the liquid sample fraction, while a micro – GC was employed for the analysis of the main gaseous products (CO, CO_2, CH_4 and H_2). An alternative tar sampling protocol was proposed, which employed the use of a cold trap (50 °C) and an isopropanol filled impinger bottle for the collection of the condensable products. The experiments were compared to heated foil reactor based pyrolysis tests within the same temperature range and heating rate, except for a slightly lower sample size (10 mg).

The Pyroprobe and adapted sampling system proved to be more efficient regarding PAH capture and quantification compared to the heated foil reactor. Naphthalene, acenaphthylene and phenanthrene were the main PAH compounds detected. The PAH yields increased with pyrolysis temperature, up to values corresponding to roughly 0.2 wt% of the overall yield at 1000 °C. From the results it was derived that PAH evolution is mainly a product of secondary decomposition of primary tar, since the char yield stabilized for higher temperatures and the yields of CO, H_2 and CH_4 increased. Overall mass balance closure values were around 80 wt% on average. Char and gas yields were determined with high reproducibility, however gravimetric liquid analysis lacked due to the inability to gravimetrically measure the yield condensing in the impinger bottle. Future work is aimed on improving on this particular aspect. Overall, the alternative tar sampling system proposed was successful in the quantification of PAH from biomass fast pyrolysis experiments offering increased flexibility, accuracy and practicality of use.

1. Introduction

Concern around environmental changes, the future depletion of conventional fossil fuel reserves as well as the ever increasing need for energy self – reliance and the global concern around environmental change caused by their use, have made heat and power generation from alternative and sustainable resources a primary research focus worldwide. Biomass is such a resource, constituting a potentially clean and renewable fuel, while being the third fuel resource worldwide, after coal and oil, in terms of abundance. Thermochemical conversion of biomass can be employed for heat, power, chemicals and fuels production. Pyrolysis, torrefaction, gasification, combustion and hydrothermal carbonization or liquefaction are considered as the major employed thermochemical conversion methods [1]. Pyrolysis is the thermochemical process of biomass decomposition, either in the absence of an oxidation medium, or with a minor amount which does not enable gasification to an appreciable extent [2]. Pyrolysis generates char, bio – oil and gases, depending on the reactor's operational regime. Pyrolysis is also a sub-process of solid fuel gasification and tar formation therein. During gasification, primary and secondary pyrolysis reactions occur among other reactions such as the water – gas shift reaction and char oxidation [3]. Biomass gasification is receiving a lot of attention as a route for (large-scale) energy conversion. However, the presence of tar in the product is linked to several issues such as condensation, formation of tar aerosols and polymerization for the formation of more complex structures. Such structures can damage process

---

[*] Corresponding author.
E-mail address: C.Tsekos@tudelft.nl (C. Tsekos).

https://doi.org/10.1016/j.jaap.2020.104802
Received 2 December 2019; Received in revised form 14 February 2020; Accepted 24 February 2020

equipment including engines and turbines [4]. The amount and nature of the produced tars depend both on the operational parameters and on the type of the biomass feedstock. Therefore, the study of a biomass feedstock's tar production potential is essential for its successful application in gasification applications.

Tar is a complex mixture of oxygenated organic compounds, 1–5 – ring aromatic hydrocarbons and complex polycyclic aromatic hydrocarbons. According to the EU/IEA/US-DOE meeting on tar measurement protocol (Brussels, 1998), the components of thermochemical conversion products with a molecular weight higher than benzene are defined as tars [5]. In the present work however, the first definition is going to be used. Tars are produced primarily through depolymerisation during pyrolysis and their formation depends greatly on the reaction conditions. At intermediately high temperatures, secondary reactions take place in the gas phase converting the oxygen-containing tar compounds produced primarily to light hydrocarbons, aromatics, oxygenates and olefins. Subsequently, higher hydrocarbons and larger polycyclic aromatic hydrocarbons are formed [6]. Polycyclic aromatic hydrocarbons (PAH) are ubiquitous environmental pollutants that are formed from natural and anthropogenic sources [7]. Low molecular weight PAHs (less than four benzene rings) are acutely toxic, while high molecular weight PAHs are mutagenic and carcinogenic [8]. They are considered as by – products of high temperature pyrolysis and incomplete combustion reactions [9]. Tars can be broadly classified into four main categories: primary, secondary, alkyl tertiary and condensed tertiary tars. Primary tars are produced during primary pyrolysis (200 °C – 500 °C) and include cellulose – derived products such as levoglucosan, hydroxyacetaldehyde and furfurals, along with analogous hemicellulose-derived products and lignin derived methoxyphenols. Secondary tars mainly include phenolics and olefins and are produced from the thermal cracking of the primary tars at temperatures higher than 500 °C. The class of alkyl tertiary tars includes methyl derivatives of aromatics, such as methylacenaphthylene, methylnaphthalene, toluene and indene, while the condensed tertiary tars class includes PAHs (naphthalene, acenapthylene, anthracene/phenanthrene, pyrene, etc.). Tar products belonging to those classes appear at pyrolysis temperatures higher than 650 °C and 750 °C, respectively [10]. Another tar classification scheme is proposed in [11] based on the solubility and condensability of the tar compounds instead of their reactivity. According to this scheme, tars can be divided into the following groups: GC – undetectable tars, heterocyclic tars which contain hetero atoms along with highly water soluble compounds (pyridine, phenol, cresols, etc.), light aromatic tars including light hydrocarbons with a single ring (toluene, ethylbenzene, xylenes and styrene), light polyaromatic tars, which are two- or three-ring compounds (indene, naphthalene, methylnaphthalene, biphenyl, acenaphthalene, fluorene, phenanthrene and anthracene) and heavy polyaromatic tars such as fluoranthene, pyrene and chrysene which have more than three rings. Among these classes light polycyclic tars condense at low temperatures while heavy polycyclics condense at high temperatures, both at low concentrations [11]. Consequently, the use of an appropriate configuration of the tar sampling method is essential for the accurate determination of the tar production spectrum.

In processes such as gasification for the production of producer gas or upgraded syngas and fast pyrolysis, which is mainly focused on bio – oil production, rapid heating rates are employed (higher than 100 °C/s). As a result, the investigation of tar formation under such conditions requires the use of reactors that can ensure such heating rates and the use of appropriate tar sampling techniques. Typical analytical pyrolyzers that are used in such experimental studies include furnace type of pyrolyzers, heated foil reactors, Curie – Point/Pyroprobe reactors, entrained flow/drop tube reactors, as well as small scale fluidized bed reactors [12,13]. In furnace type of pyrolyzers, the (small particle size) sample is introduced into a preheated zone rapidly. In Curie – point pyrolyzers, the samples are placed on ferromagnetic wires or small sheets and they undergo pyrolysis at the Curie temperature of the ferromagnetic alloys [13]. Heated foil reactors, pyrolyze a thin disk of particles in an electrically heated wire mesh, while the heating rate and holding time are controlled by the proper adjustment of the current to the screen [12]. Pyroprobe reactors perform platinum filament heated pyrolysis, where the temperature of the filament surrounding the sample is controlled by variation of the voltage drop [14]. Drop tube furnaces are mostly vertical and down – fired and the samples are introduced in pulverized form. Entrained flow reactors are a variation of the drop tube furnace where the fuel particles are entrained in a carrier gas along the axis of the furnace into a flowing preheated gas stream. All these types of pyrolyzers can achieve maximum temperatures above 1400 °C and appropriate heating rates for the conduction of fast or flash pyrolysis experiments [15]. Tar sampling from such instruments is based on cold trapping techniques followed by solvent absorption. The obtained volatiles can be analysed by the means of high – performance liquid chromatography (HPLC), size – exclusion chromatography – UV, gas chromatography (GC) – flame ionisation detection (FID) or GC – mass spectrometry (MS) [16]. In Tables 1, the reader can find a brief overview on some tar sampling methods for PAH detection from fast pyrolysis reactors.

Pyroprobe reactors in particular have been widely employed in the investigation of the pyrolysis characteristics of biomass species. Analysis of the produced volatiles is usually performed by means of GC - MS [23–31]. This choice however, creates an obstacle regarding the quantification of PAH species produced during pyrolysis. The main reason is that during devolatilization/pyrolysis most condensable gases are absorbed in the pyroprobe trap. By increasing the local temperature, desorption of the tars takes place at a maximum temperature of 350 °C. This temperature is not sufficient for the desorption of all the PAHs and especially the heavier ones. For example, the boiling point of pyrene and fluoranthene are 393 °C and 383 °C, respectively [32]. Furthermore, limitations are imposed by the maximum GC inlet temperature and the maximum temperature of the GC line interface (typically below 300 °C and 200 °C, respectively [33]). Heavy PAHs can also recondense on the GC column under the aforementioned conditions. In general, quantitative results on the production of PAH cannot be obtained through PY – GC/MS pyrolysis [34]. Only qualitative results can be obtained, through the determination of the total calibrated chromatographic peak areas for several experiments performed at different temperatures with the same sample mass [35].

In this paper, PAH formation during the fast pyrolysis of woody biomass within a high temperature range (500 °C to 1000 °C) is investigated. An additional purpose of this study is to present a fast and accurate method for PAHs sampling and quantification from pyrolysis experiments in a Pyroprobe reactor. More specifically, condensation of the produced PAHs was achieved by the coupling of the built – in trapping system of the Pyroprobe with an isopropanol filled condenser at room temperature. The obtained tars, dissolved in isopropanol, were analysed using an HPLC for the quantification of each PAH content, without the need for a solvent evaporation step, Besides the time and accuracy benefits of this method, the simultaneous sampling of the non – condensable pyrolysis products is possible. Thus, at least satisfactory mass balance values can be obtained and links between tar and permanent gases evolution can be investigated. Moreover, the decoupling of the Pyroprobe reactor from a GC/MS system allows the conduction of experiments with oxidizing agents such as air, oxygen and CO_2, although such attempts were not part of this study. Overall, this method offers a more complete determination of a biomass feedstock's fast devolatilization characteristics and the effects of operational parameters on the products' nature and distribution. The results were compared to those obtained from a heated foil reactor at the same process conditions. Significant differences, however, exist between the two reactor systems related to heat and mass transfer characteristics, sample size, tar sampling procedure, etc.. Considering the limitations in both cases (e.g. sample size – see section 2.2), both reactor systems were used in such a way as to ensure yields relevant to the relatively

Table 1
PAH capturing and analysis methods from pyrolysis reactors reported in literature.

Feed	Pyrolysis reactor	Temperature (°C)	Heating rate	Tar sampling method	Post sampling	Tar analysis instrument	PAH species detected	Ref.
Xylan, cellulose, lignin	Fixed bed reactor	800	350 °C/min	Air and dry ice condensers	Washing by ethyl acetate	GC/MS	2, 3 and 4 ring PAHs	[17]
Municipal solid waste	Fixed bed reactor	800	350 °C/min	Air and dry ice condensers	Removal of aliphatic compounds and part of the aromatic tar fraction by washing with hexane. Remaining aromatics were obtained through ethyl acetate washing. Aliphatic and aromatic compounds were separated with a silica – alumina sorbent packed column.	GC/MS	2, 3 and 4 ring PAHs	[18]
Sawdust	Continuously fed drop-tube furnace	600 – 1400	n.a.	One sampling probe with a quartz filter and three 2-propanol filled impinger bottles; two at room temperature and one placed in a methanol – CO2 ice bath	Evaporation at room temperature for 20–30 h to constant weight. Heavy tars condensed in the sampling line were added to this residue after washing with tetrahydrofuran.	Identification by GC/MS and quantification by GC-FID	2, 3 and 4 ring PAHs	[19,20]
Cellulose, pectin, chlorogenic acid	Quartz tube reactor	700 - 850	n.a.	Cambridge pad	Extraction with methanol from the pad. The reactor was rinsed with methanol.	GC/MS	2, 3 and 4 ring PAHs	[9]
Wood chips	Quartz tubular reactor	700	n.a.	1) Two frit – less ice cooled impingers, immerse in ice and liquid N_2 and 2-propanol. Another two impingers with glass frit immerse in ice. 2) SPA tubes (Carbotrap 300 pacted within stainless steel tubes) heated at 350 °C	Injection of internal standards	GC/MS Thermal desorption with capillary GC/MS	2 and 3 ring PAHs	[16]
Acetylene	Quartz reactor	800 - 1000	n.a.	Light PAHs were retained as they passed through a fine tube filled with XAD-2 resin. Heavy PAHs were adsorbed on the produced soot or on the reactor walls or they were collected using quartz fibre filters.	Soxhlet extraction followed by PAH concentration by rotary evaporation and micro-concentration under nitrogen stream.	GC/MS	2, 3 and 4 ring PAHs	[21]
Poplar wood	Pyroprobe reactor	500	20 °C/ms	1) Solid phase extraction (Py-SPE). Silica gel was introduced to a glass tube packed with glass wool and conditioned with n-hexane. 2) Solid phase micro-extraction (Py-SPME) through a carboxen/polydimethylsiloxane fibre placed at the exit of the pyrolysis chamber.	1) The trapping apparatus was spiked with a surrogate PAH mix, rinsed with n-hexane and the solvent was collected in a vial after passing through the silica gel. The solution was subsequently blown down under N_2. 2) The fibre was introduced into an ammonia aqueous solution under magnetic stirring for 15 min and then dried under N_2 flow.	GC/MS	Up to 6 ring PAHs	[22]

Table 2
Proximate and ultimate analysis of waste softwood [36].

	a.r.	d.b.	daf
Moisture[a] (wt%)	7.9	–	–
Ash[a] (wt%)	0.7	0.8	–
VM[a] (wt%)	72.1	78.3	78.9
FC[a] (wt%)	19.3	21.0	21.1
C (wt%)	45.6	49.5	49.8
H (wt%)	4.7	5.0	5.1
N (wt%)	0.5	0.5	0.5
S (wt%)	0.04	0.04	0.04
O[b] (wt%)	36.5	39.6	39.9
HHV (MJ/kg)	18.1	20.6	20.7

[a] calculated by TGA.
[b] calculated by difference.

high heating rate industrial application cases for all product fractions (gas, char, tar), which would also positively affect the identification of its individual gaseous and tar (in this case PAH) compounds afterwards. Therefore, the purpose of any comparison of the two performed, is to highlight the differences in PAH quantification from biomass fast pyrolysis by following two different procedures.

2. Materials & methods

2.1. Proximate and ultimate analysis of the fuels

Raw biomass used in this work was supplied by the Dutch company Synvalor. In particular, a waste softwood mixture, a by-product of furniture manufacturing was used as a feedstock. Prior to the experiments the biomass was ground and sieved to powder with particle size < 90 μm. Proximate and ultimate analysis of the wood is provided in Table 2. Analytical description of the procedures followed for the analysis, as well as the sugar and biochemical composition of the feedstocks can be found in [36].

2.2. Apparatus and experimental procedure

The fast pyrolysis experiments were conducted on a CDS Pyroprobe Model 5200, equipped with a ½”coil probe, able to house a quartz tube with maximum capacity of approximately 300 mg of sample. Fig. 1 presents a schematic overview of the equipment and the experimental procedure. This configuration allows higher biomass loading, compared to traditional Py-GC/MS applications where the typical biomass loading is 2 – 3 mg. In this way the inaccuracies and uncertainties during product collection and determination can be significantly reduced. For each experiment, a sample of approximately 30 mg of woody biomass was placed in the middle of the quartz tube, with the support of some quartz wool in both ends. This sample size was selected in order to avoid the introduction of heat and mass transfer limitations imposed by larger sample sizes. At the same time, this sample size is considered large enough to lead to the production of considerable yields of the products investigated.

The coil probe, loaded with the quartz tube containing the sample was introduced in the Pyroprobe interface. The interface was heated from an initial temperature of 50 °C–300 °C at a heating rate of 100 °C/min. Afterwards, the coil was heated to the desired pyrolysis temperature which was maintained for 10 s, with a heating rate of 600 °C/s. It has to be noted that the actual temperature inside the quartz tube differs from the one that is set for the probe coil. According to the manufacturer, the difference is approximately 100 °C, however after measurements with a thermocouple inside the sample quartz tube performed by the authors, it was found that the difference was actually higher, especially for temperatures above 600 °C. As a result, the filament temperature was set accordingly for each experiment. For example, in order to achieve a temperature of 800 °C for the sample's pyrolysis, the filament temperature needs to be set at 1008 °C. It should be noted that the temperature correction regards only the quartz tube effect and not the effect of the sample's presence in the tube, since such measurements cannot be conducted in the current setup. Furthermore, due to the low thermal conductivity of the quartz tube, the actual heating rate that the sample experienced is also expected to be lower than the imposed 600 °C/s heating rate of the probe coil (approximately 450 °C/min). The conduction of experiments with increased holding times (up to 12 s), in order to compensate for the lower actual heating rate, did not lead to any differences in the experimental results. The conditions were chosen to match previous experiments with the same feedstock on a heated foil reactor [36] for direct comparison purposes. Nitrogen (purity 99.999 %) was used as a purge gas at a constant flow of 10 mL_n/min using a flowmeter. The pyrolysis vapours flowed from the quartz sample tube to the trap through the valve oven which was kept at 325 °C. The trap consisted of a quartz tube (114 mm L, 4 mm I.D.) equipped with a glass frit in order to facilitate aerosol condensation. The trap was heated with a heating jacket at 50 °C because of the high temperature in the oven upstream the trap (325 °C). The majority of condensable products (tars) condensed in the trap. However, an additional liquid trap was connected downstream this quartz tube trap in order to ensure the condensation of lighter tar species. The liquid trap consisted of an impinger bottle filled with 2 mL of 2-propanol (IPA) provided by Sigma Aldrich (99.9 % purity). At the exit of the liquid trap gases were collected in a syringe with a freely moving piston for subsequent analysis by micro-GC. The quartz trap was washed with an additional 3 mL of IPA and the resulting solution was then mixed with the constituents of the liquid trap for the subsequent HPLC analysis. At the end of the experiment, the char product and the liquid product (tars and with pyrolytic water) that condensed in the quartz trap were

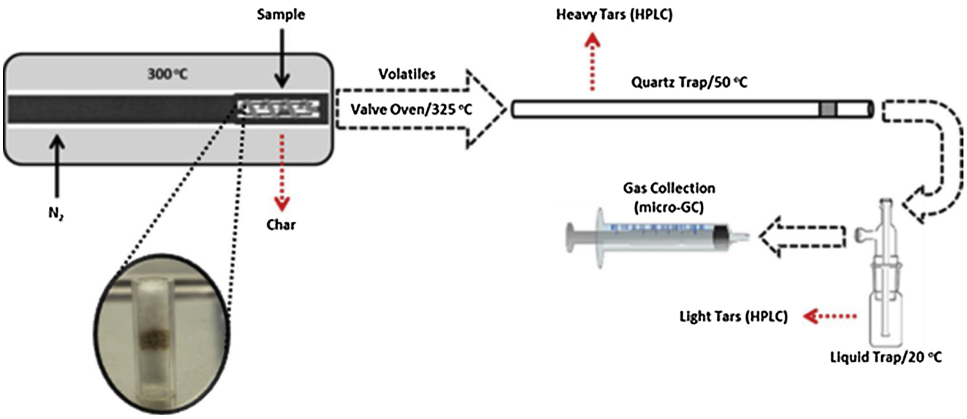

Fig. 1. A schematic overview of the experimental procedure and product sampling methods that were followed in the conduction of the pyrolysis experiments.

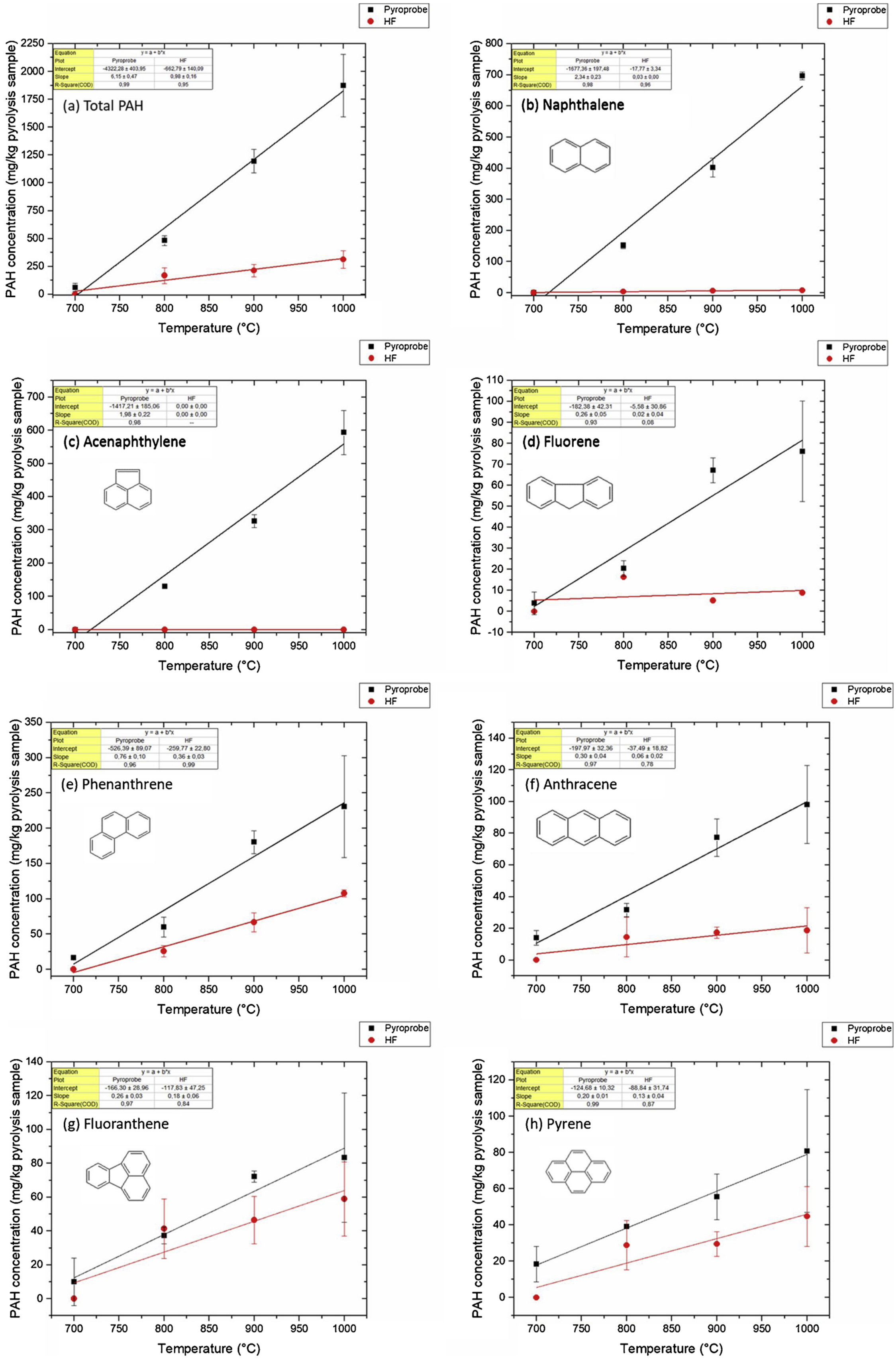

Equation	y = a + b*x	
Plot	Pyroprobe	HF
Intercept	-4322,28 ± 403,95	-662,79 ± 140,09
Slope	6,15 ± 0,47	0,98 ± 0,16
R-Square(COD)	0,99	0,95

Equation	y = a + b*x	
Plot	Pyroprobe	HF
Intercept	-1677,36 ± 197,48	-17,77 ± 3,34
Slope	2,34 ± 0,23	0,03 ± 0,00
R-Square(COD)	0,98	0,96

Equation	y = a + b*x	
Plot	Pyroprobe	HF
Intercept	-1417,21 ± 185,06	0,00 ± 0,00
Slope	1,98 ± 0,22	0,00 ± 0,00
R-Square(COD)	0,98	--

Equation	y = a + b*x	
Plot	Pyroprobe	HF
Intercept	-182,38 ± 42,31	-5,58 ± 30,86
Slope	0,26 ± 0,05	0,02 ± 0,04
R-Square(COD)	0,93	0,08

Equation	y = a + b*x	
Plot	Pyroprobe	HF
Intercept	-526,39 ± 89,07	-259,77 ± 22,80
Slope	0,76 ± 0,10	0,36 ± 0,03
R-Square(COD)	0,96	0,99

Equation	y = a + b*x	
Plot	Pyroprobe	HF
Intercept	-197,97 ± 32,36	-37,49 ± 18,82
Slope	0,30 ± 0,04	0,06 ± 0,02
R-Square(COD)	0,97	0,78

Equation	y = a + b*x	
Plot	Pyroprobe	HF
Intercept	-166,30 ± 28,96	-117,83 ± 47,25
Slope	0,26 ± 0,03	0,18 ± 0,06
R-Square(COD)	0,97	0,84

Equation	y = a + b*x	
Plot	Pyroprobe	HF
Intercept	-124,68 ± 10,32	-88,84 ± 31,74
Slope	0,20 ± 0,01	0,13 ± 0,04
R-Square(COD)	0,99	0,87

Fig. 2. PAH evolution during pyrolysis (600 °C/s, 10 s holding time) of wood at different temperatures, comparison between pyroprobe and heated foil (HF).

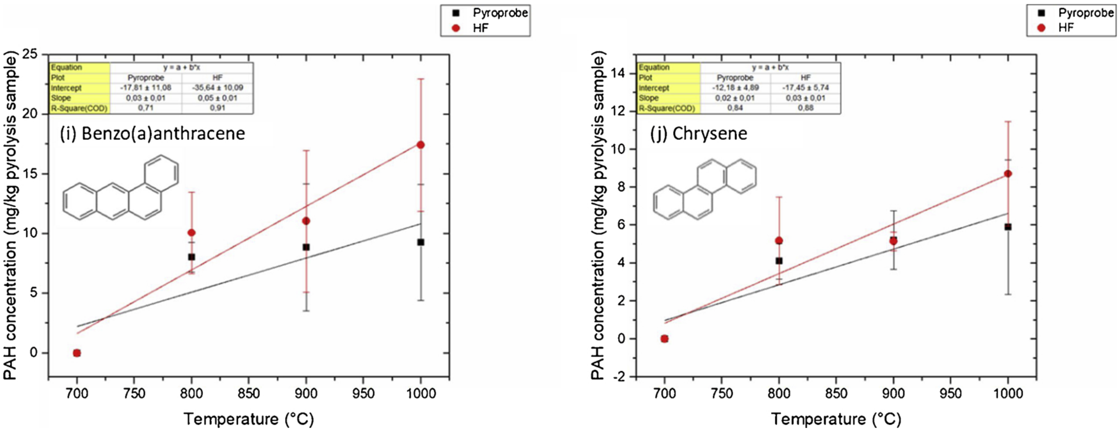

Fig. 2. (*continued*)

determined gravimetrically by weighing the sample quartz tube and the quartz trap, respectively. All experiments were performed in triplicate.

The heated foil reactor employed was coupled with an FTIR for the simultaneous analysis of the product gases. A detailed schematic of the reactor and the overall procedure can be found in [36]. Briefly, the biomass sample was ground and sieved to particle sizes below 90 μm and subsequently, 10 mg were compressed into a tablet (2.5 mm diameter, 0.7 mm thickness) by using a pellet press (force of 2 t). The sample size employed is limited to 10 mg, since for larger sample sizes, the increased thickness of the tablet would impose significant temperature gradients in the sample, as it was found by the authors in [37]. The tablet was then placed on the stainless steel foil and the reactor was purged with N_2 (purity 99.999 %) in order to create an inert atmosphere. No temperature correction was employed in the case of the heated foil experiments, since the thermocouple of the instrument is located on the plate were the sample is placed. Subsequently, the sample was heated to the final pyrolysis temperature (500–1000 °C) for 10 s at a heating rate of 600 °C/s. A circulation pump was used for carrying the product gases to the FTIR for analysis. After the gas analysis, the reactor was cooled down by a N_2 stream and the remaining char was retrieved from the foil and measured gravimetrically. Glass wool was placed at the outlet of the main chamber (before the circulation pump) to serve as a tar trap. The tar trapped in the glass wool filters was washed with DCM (dichloromethane) and mixed with the tar obtained from the reactor's walls and lid (also washed with DCM). After filtering, the total solution was subjected to DCM evaporation at room temperature in a fume hood and the final total tar yield was determined gravimetrically. All experiments were performed in triplicate.

2.3. *Analysis of the products*

Tars from pyrolysis experiments were analysed by means of a high performance liquid chromatograph (HPLC) supplied by KNAUER System. Separation was achieved on an UltraSep ES PAH QC, 60 × 2.0 mm column, with a mobile phase of water/acetonitrile at a flow rate of 0.5 ml/min. The analysis temperature and analysis time were 25 °C and 17 min, respectively. Determination of tar composition was accomplished with a combination of ultraviolet-visible light (UV) and fluorescence detectors. According to the US Environmental Protection Agency (EPA) [38], the UV detector is recommended for the determination of naphthalene, acenapthylene, acenaphthene, and fluorene while the fluorescence detector is recommended for the remaining PAHs. The UV detector wavelength was set at 254 nm. In the fluorescence detector, unlike in the UV detector, the wavelength varies with time during each experiment. The fluorescence excitation (EX) and emissivity (EM) wavelengths were set for the individual groups of PAHs as: EX-275 nm, EM-325 nm for naphthalene, acenaphthene and fluorene; EX-255 nm, EM-375 nm for phenanthrene and anthracene; EX-270 nm, EM-420 nm for fluoranthene and pyrene; EX-275 nm, EM-383 nm for benzo(a)anthracene and chrysene; EX-295 nm, EM-410 nm for benzo(b)fluoranthene, benzo(k)fluoranthene and benzo(a)pyrene; EX-301 nm, EM-420 nm for dibenzo(a,h)anthracene and benzo(g,h,i) perylene and finally EX-304 nm, EM-501 nm for indeno(1,2,3-cd) pyrene. Due to the limited amount of strongly fluorescent compounds, the fluorescence detection is highly selective.

A certified PAH standard mixture (SS EPA 610 PAH Mix $100 - 2000$ μg/ml methanol : methylene chloride 1:1) was supplied by Sigma Aldrich for calibration of the HPLC system. The calibration was carried out using the standards at 7 different concentrations. Each calibration standard was injected three times in order to check the analysis repeatability and the calibration curve was prepared by considering the whole set of injections. The correlation factor obtained after the calibration procedure was $R^2 > 0.99$ for all of the PAH compounds under investigation. The fluorescence detector, being very sensitive concerning PAH analysis, can detect very low concentrations. The system was calibrated with a lowest concentration limit of 0.2 μg/ml.

Gas analysis for the pyroprobe experiments was performed on a Varian μ-GC CP4900. Separation of H_2, CO, CO_2 and CH_4 was achieved on a 1 m CP − COX column and detection and quantification by a TCD detector with Argon used as carrier gas. For the heated foil experiments, a Thermo Nicolet NEXUS 6700 FTIR was used. The FTIR was calibrated for CO_2, CO, CH_4 and H_2O detection and quantification. The resolution was 0.25 cm^{-1} and 3 scans were averaged every 9 s for a total time of 3 min.

3. Results & discussion

3.1. *Influence of pyrolysis temperature on PAH evolution*

The total PAH along with the main individual PAH compounds found in the product tar/oil from wood pyrolysis (600 °C/s, 10 s holding time) at different temperatures from both analytical pyrolyzers (pyroprobe – PP and heated foil reactor – HF) are depicted in Fig. 2. Appreciable quantities of PAHs were found only at peak pyrolysis temperatures exceeding 700 °C.

In the case of the PP experiments, the total PAH yield increased from 60 mg/kg at 700 °C to approximately 1900 mg/kg at 1000 °C. The total PAH yield, as can be seen in Fig. 2 (a), was significantly higher for the pyroprobe experiments in all temperatures examined and this difference increased for increasing temperature. In particular, no PAHs were detected for the HF experiments at 700 °C while the corresponding yield for the PP was 60 mg/kg of sample. For 800 °C, the PP experiments resulted in almost twice the PAH yield compared to the HF tests, while for 900 °C and 1000 °C PP PAHs were approximately 4.5 and 5 times higher, respectively. The differentiation between the two experimental procedures arises mainly from the effectiveness of light PAH capture. Light polyaromatic tars include two and three ring compounds and have the tendency to condense at intermediate to low temperatures even at very low concentrations. On the other hand heavy polyaromatic compounds (larger than three rings) condense mostly at high temperatures [11].

Naphthalene was the most abundant PAH detected in the PP experiments. The difference between the two methods was significant and it increased with increasing temperature, since the naphthalene yield increased as well. Specifically, the naphthalene yield was roughly 40, 60 and 90 times higher for the PP experiments in comparison to the HF tests at 800, 900 and 1000 °C, respectively (Fig. 2 (b)). In the case of the HF experiments, fluoranthene at 800 °C and phenanthrene at 900 °C and 1000 °C were the PAH produced at the highest concentrations. It is interesting to note, that despite this fact, the fluoranthene yields of the two reactors were comparable at 800 °C (41 mg/kg – HF versus 37.4 mg/kg – PP) while PP pyrolysis produced more than two times higher phenanthrene yields at 900 °C and 1000 °C.

Another major difference between the two reactor systems, was the absence of acenapthylene from the HF pyrolysis products, while in the case of PP it constituted the second higher PAH specie yield detected. In general, the HF reactor underperformed in comparison to the PP in terms of light polyaromatic compounds production (naphthalene, acenaphthylene, fluorene, phenanthrene and anthracene). As it can also be seen in Fig. 2 (d–f) the yields of fluorene were on average 7.6 times higher for PP experiments, the ones of phenanthrene 2.4 times higher and anthracene's approximately 4 times higher. These differences correspond to 800 °C, 900 °C and 1000 °C, since at 700 °C, no PAH where detected at all for the HF. One potential explanation for the less successful light PAH sampling from the HF, lies in the employment of the evaporation step in those experiments. It is very likely, that lighter PAH species evaporated as well during the DCM evaporation, causing these differences with the PP experiments. The situation however was different for heavier PAH compounds. In particular, some species that were captured in the HF experiments were not present in the PP ones. Namely, benzo(b)fluoranthene, benzo(k)fluoranthene, benzo(a)pyrene and indeno (1,2,3-cd)pyrene were detected only in the HF tar samples. However, their concentration was particularly low, ranging from 14.6 mg/kg of wood for benzo(a)pyrene at 1000 °C to as low as 2.6 mg/kg of wood for benzo(b)fluoranthene at 800 °C. Regarding the rest of the species, as can also be observed in Fig. 2 (g–j) the differences were minimal between the two reactors, with the HF test results having a slight edge over the PP results for benzo(a)anthracene and chrysene. Heavy polyaromatic tars can condense at high temperatures and at low concentrations as it was mentioned earlier. This can potentially explain the differences between the two reactors, since tar sampling for the HF was performed closer to the sample in comparison to the PP. It is possible that part of the heavier PAH condenses on the tube in the PP oven, or escapes the tar sampling system due to its low concentration [39,40].

Limited information is available in literature concerning PAH formation at high pyrolysis temperatures, since pyrolysis is not usually employed at temperatures higher than 800 °C. Morf et al. [41] conducted homogeneous tar conversion experiments by initially pyrolysing fir/spruce wood chips at 380 °C and subsequently guiding the evolved gases to the tar conversion zone were they remained for less than 0.2 s. The naphthalene yield obtained from those experiments ranged between 200 mg/kg at 830 °C and 1167 mg/kg at 990 °C. These values are comparable to the results presented in this study, since they also regard the secondary conversion of primarily formed tars in a continuously fed reactor. Zhou et al. performed fast pyrolysis of xylan, cellulose and dealkaline lignin in a fixed bed reactor at 800 °C [17,18]. Tar sampling was performed with two air and dry ice cooled condensers and analysed by GC/MS. The authors reported total PAH yields of 156.2 mg/kg, 59.1 mg/kg and 541 mg/kg for xylan, cellulose and lignin, respectively, which were also close to the results presented here. The results also compare well to the work previously published by the same group [42], where using the same type of PP reactor wood residues and ash wood was pyrolysed, producing a PAH yield ranging from 291 mg/kg to 1189 mg/kg and 143 mg/kg to 1549 mg/kg between 800 °C and 1000 °C, respectively. The yields of acenaphthalene, fluorene, phenanthrene, anthracene and pyrene in the present work are also consistent with the findings of Brage et al. at [43] although somewhat lower i.e. fluorene yield of 276 mg/kg at 900 °C versus 67.18 mg/kg for PP. On the contrary, the naphthalene yields reported were three and four times higher at 800 °C and 900 °C, respectively, compared to the PP results. Brage et al. conducted hardwood pyrolysis at 700 °C and steam cracking of the produced gases between 700 °C and 900 °C. Tar sampling was performed through a series of Liebig condensers and cryogenic traps, the latter immersed in ice-acetone and dry-ice-acetone. The tars were extracted by washing with dichloromethane and acetone and the samples were introduced in a GC—MS, following solid-phase extraction. It is apparent, that steam cracking facilitated the decomposition of primary and secondary tars for the production of PAH. Furthermore, experiments of Dufour et al. presented in [16] also yielded significantly higher amounts of naphthalene, acenaphthylene and phenanthrene compared to the present study. These experiments were performed with wood chips as feedstock in a quartz tubular reactor and the sampling procedure was described earlier in the introduction. A possible reason for the observed differences is the presence of a gas cracking/conversion zone in the Dufour et al. reactor which lies right after the biomass sample location and before the SPA sampling point. According to Cypres [44], the primary mechanism of phenol cracking is the simultaneous formation of CO and cyclopentadiene, with dibenzofurane formation being the second primary reaction. Further cracking of cyclopentadiene leads to benzene, toluene, indene and naphthalene formation along with H_2. Yu et al. [45], proposed a second pathway to PAH formation. According to the authors, benzene generates bicyclic or polycyclic PAHs through the abstraction of hydrogen atoms, the addition reaction of ethylene molecules or by the benzene ring condensation reaction of PAHs. Therefore, there is the possibility that phenol or benzene cracking can lead to higher PAH yields in the reactor of Dufour et al.. Finally, it is interesting to note that in both Brage's and Dufour's work, pyrene and phenanthrene, were the heavier PAHs reported, respectively, in contrast with the present work which reports PAH until indeno (1,2,3-cd)pyrene. Heavy PAH, are generally found in low concentrations in biomass tars, as it also apparent here, but their detection and quantification is crucial for the scale – up of any pyrolysis or gasification process.

The present study reports a wider range of PAH compared to other studies. In particular, only naphthalenes are reported in [46] for Jatropha fast pyrolysis at 500 °C for 30 s in a pyroprobe – GC/MS system. In [47], again for Pyroprobe – GC/MS pyrolysis of sawdust between 500 °C and 800 °C, only naphthalene, phenanthrene and anthracene are reported. Trubetskaya et al. in [48], report 14 PAH in total (up to $C_{17}H_{12}$) from lignocellulosic compounds pyrolysis at a drop tube reactor between 800 °C and 1250 °C. However, in order to achieve this, before the quantitative analyses in a GC – FID the tar compounds were annotated using a dual detector system (GC/MS – GC-FID). Numerical comparison with the previously mentioned studies was unfortunately not possible since either area or mol percentages were reported.

Some interesting observations can also be made by studying the distribution of the PAH species between the quartz and the impinger trap for the PP reactor. In Fig. 3 (a), it becomes apparent that at 800 °C, a temperature associated with lower PAH concentrations (compared to higher temperatures), the vast majority of PAHs tend to condense in the first trap (quartz) of the system. Less than 15 wt% of each of two or three ring compounds (light polyaromatics) was found in the impinger trap. However, a major shift is observed at 1000 °C, especially for the two major PAH species formed (naphthalene and acenaphthylene) (Fig. 3 (b)). At this temperature, roughly 95 wt% and 80 wt% of the naphthalene and acenaphthylene yields were found present in the

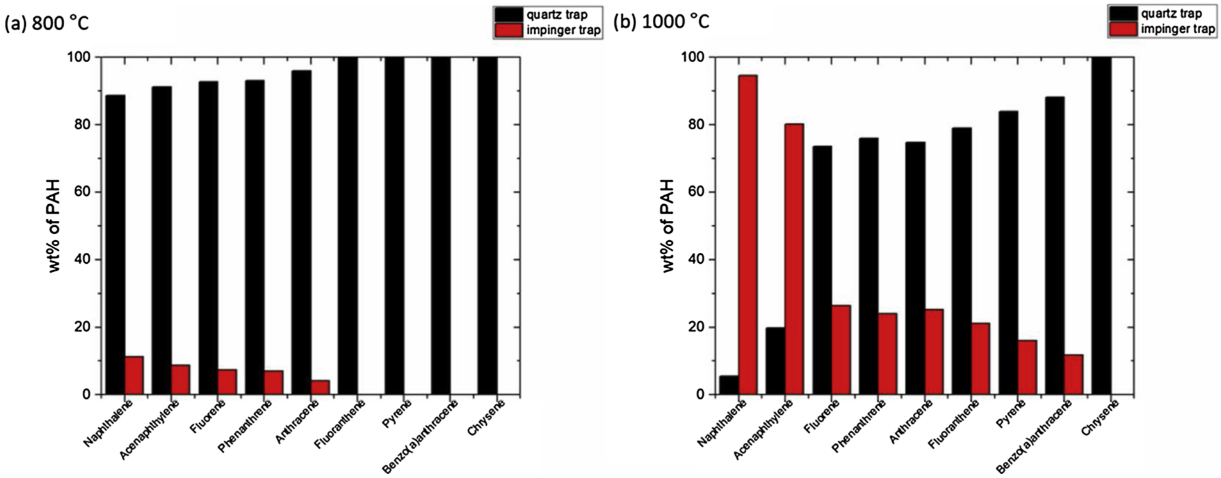

Fig. 3. PAH condensation on quartz and liquid traps from wood pyrolysis on PP (600 °C/s, 10 s holding time) at (a) 800 °C and (b) 1000 °C.

impinger trap, while the presence of the other PAHs in the liquid (impinger) trap also increased (with the exception of chrysene). These data suggest that a cold zone is sufficient in order to trap the major fraction of PAHs formed at lower temperatures (e.g. 800 °C) where total PAH yield is relatively low (approximately 500 mg/kg at 800 °C). However, at higher temperatures (e.g. 1000 °C) and higher PAH concentrations (approximately 1900 mg/kg at 1000 °C) the cold trap is not sufficient for effective condensation of PAHs, especially light PAHs (2 and 3 rings). This can be also attributed to a local increase of the temperature of the cold trap, due to the increase of the temperature of the product gas flow.

3.2. Gravimetric liquid and char from PP and HF reactors

The char and liquid yields of the PP and HF reactors are presented as percentages of the initial biomass feed in Fig. 4. Regarding the char product, very similar trends can be observed in both cases. Char production decreases with increasing temperature until 700 °C for the PP, before attaining a near-constant profile for higher temperatures. The corresponding temperature for the HF was 800 °C. Liquid production peaks for both cases at 600 °C and subsequently decreases until 800 °C, maintaining a fairly constant yield above this temperature. The char yield reduction with the increase of the temperature, is the attributed to the increased primary decomposition of the biomass (hemicellulose, cellulose and lignin decomposition) as well as to the secondary char decomposition which mainly leads to non – condensable gases production [49]. The decrease of the liquid yield between 600 °C and 800 °C, for both the HF and PP reactor can originate from secondary cracking of liquid products to lighter volatiles (H_2, CO, CH_4, C_2H_4, etc.) despite the short residence time in the apparatus employed [50,51] or from rigorous reactions in the decomposing biomass [52]. In general, the observed char yields and their trend for increasing temperature are in good agreement with several earlier similar studies of biomass fast pyrolysis [53–56]. The same holds for the liquid yields [54–56].

The differences between the char and liquid yields from the two reactors are more pronounced in the lower temperature range. In particular, the char yields were higher for the HF reactor at 500 °C and 600 °C by ~20.6 wt% and 6.8 wt%, respectively. This can be attributed to the thermal lag in the biomass sample in heating foil reactors. The poor thermal conductivity of woody biomass and the non-distributed source of heating (foil) in heating foil reactors creates temperature gradients inside the pyrolysing sample [37]. This thermal lag is more pronounced at lower temperatures and low residence times. At temperatures higher than 600 °C the average difference was 2.2 wt% in favour of the PP. This difference can be attributed to minor inaccuracies occurring during the gravimetric determination of char yields. Higher sample mass was used in PP experiments (30 mg) compared to HF experiments (10 mg) which would reduce any inaccuracies during char yield determination. Furthermore, inaccuracies during gravimetric char yield determination should be contained at minimum in case of PP experiments, since the resultant char was weighed in the sample quartz tube originally containing the starting feedstock. On the contrary, in case of HF experiments the resultant char had to be manually removed from the foil and subsequently weighed, a procedure during which

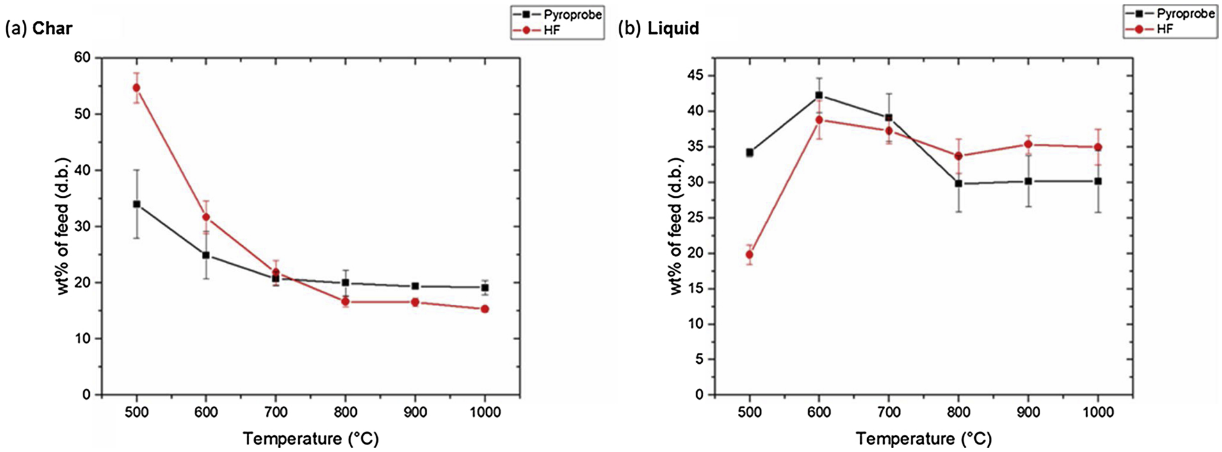

Fig. 4. Effect of pyrolysis (600 °C/s, 10 s holding time) temperature on (a) char and (b) gravimetric liquid (condensables on quartz trap) yields.

minor losses of char particles can occur.

The lower extent of devolatilization of wood sample in the HF reactor at 500 °C and 600 °C resulted in less liquid yield as expected. Nonetheless, liquid yields as determined gravimetrically were comparable at 600 °C and 700 °C for both analytical pyrolyzers (42 wt% for PP compared to 39 wt% for HF at 600 °C, 39 wt% for PP compared to 37 wt% for HF at 700 °C). At higher pyrolysis temperature (> 800 °C) the liquid yield determined gravimetrically from the HF was higher than that of PP. Considering the values of the standard deviation, the difference in this temperature range becomes less significant. However, as it was also shown in Fig. 3, at high temperatures, naphthalene and acenaphthylene, which constitute the larger fraction of the detected tars tend to condense in the impinger trap for the PP. This liquid yield is not measured gravimetrically, as it was mentioned earlier. Therefore, it is fair to assume that along with light PAHs, lighter condensables also tend to condense in the impinger, thus explaining this difference between the two methods. Overall, it can be observed that PAH compounds constitute only a very small part of the total liquid yield from the fast pyrolysis experiments (maximum 0.2 wt% at 1000 °C). Lower molecular weight compounds (i.e. levoglucosan, phenolics, olefins, etc.) as well as pyrolytic water represent the by far larger part of fast pyrolysis liquid yield. As it was also evident in the previous work published by the authors, for woody biomass fast pyrolysis in the same pyroprobe reactor, only the phenol yield at 800 °C can be 8 times higher than the total PAH yield [42].

3.3. Analysis of the product gas

The total amount of gases produced from the two reactors were similar, ranging from 12 wt% to 34 wt% for the PP and from 6.5 wt% to 33 wt% for the HF. From Fig. 5, it can be derived that the main reason for this difference is the lower amount of CO_2 produced during the HF experiments at 500 °C and 600 °C, due to the lower extent of devolatilization of biomass sample as explained earlier. Furthermore, the CH_4 yield became stable for the HF above 800 °C in contrast with the PP where the increase continued until 1000 °C. The values for CO were similar, while H_2 was not measured in the case of the HF.

It is important to notice that CO_2 is the highest yielding gas until a temperature of 700 °C for both reactors studied. Above this temperature, CO becomes the most prominent gas and as can be seen in Fig. 5 (d) and the yield of H_2 monotonously increases despite remaining at low levels overall. Keeping in mind the stable char yield and the decreasing liquid yield at temperatures above 700 °C, it can be concluded that secondary decomposition (cracking) of tar compounds is responsible for the increasing gas yield above this temperature. Primary devolatilization of the softwood sample leads to the production of mainly tar and CO_2 until 700 °C. However, the further increase of the pyrolysis temperature leads to subsequent tar decomposition, producing more CO and H_2 [50,51]. Furthermore, as it was also mentioned before, phenol and BTEX (primarily benzene) compounds can both serve as PAH precursors. The rapid increase of the H_2 yield observed here can be therefore linked to PAH formation, either through phenol cracking [45] or through the HACA sequence [41]. Finally, regarding CH_4,the steep increase of its yield from 0.2 wt% to 3.5 wt% from 500 °C to 1000 °C can also be attributed to the reforming and cracking of tar compounds [57].

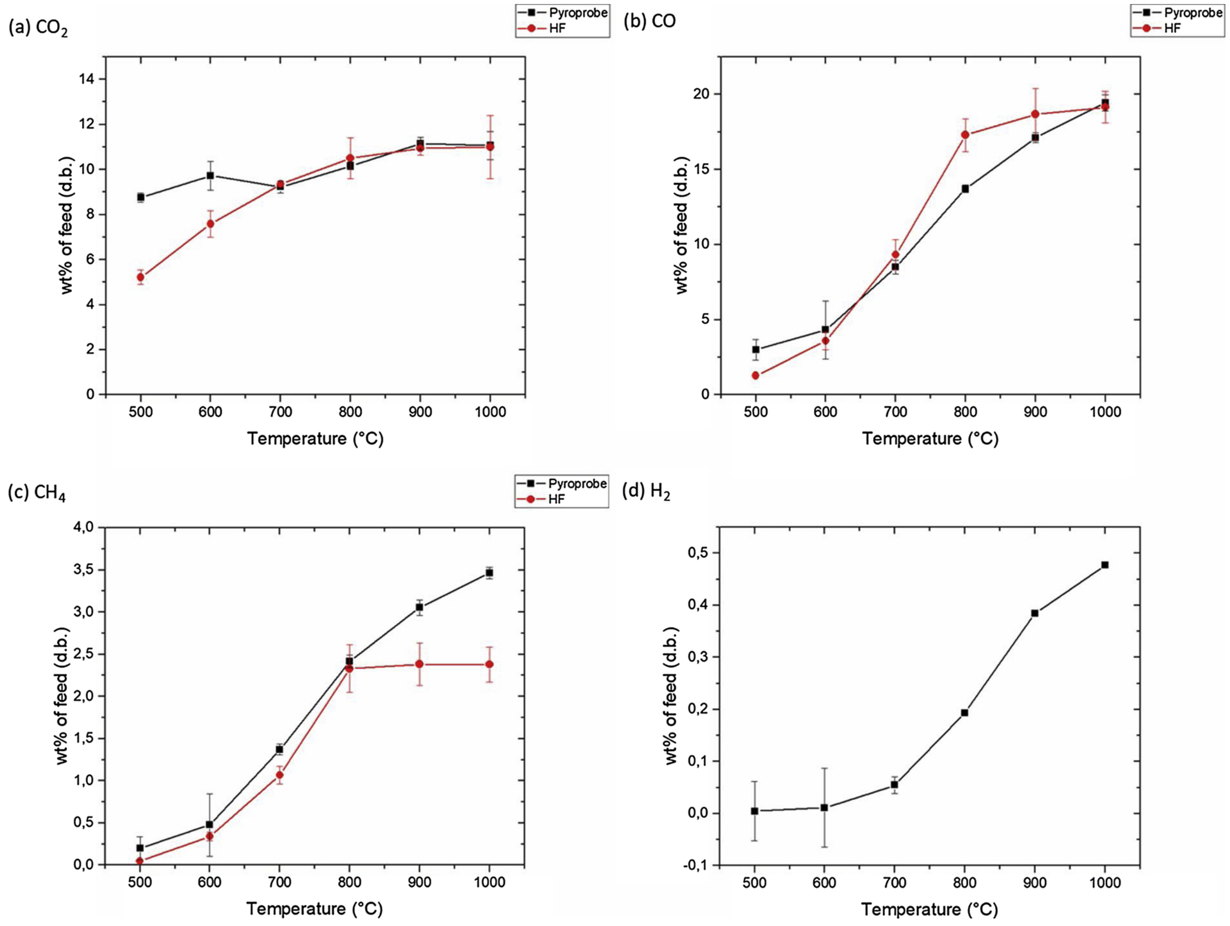

Fig. 5. Gas evolution over temperature during pyrolysis (600 °C/s, 10 s holding time) of wood: (a) CO_2, (b) CO, (c) CH_4 and (d) H_2. Comparison between pyroprobe and heated foil.

3.4. Overall mass balance of the experiments

The overall mass balance of the experiments was calculated as the summation of the individual product classes' yields (gas, liquid and char) for both the HF and PP reactors. For the PP reactor, the average mass balance closure value was 80 wt% while the corresponding value for the HF was slightly higher (81.7 wt%), but similar overall. In both cases, the mass balance closure values increased for increasing temperature. In the HF reactor mass losses can occur from the char collection especially at high temperatures since the sample is not contained in the heating system, unlike in the case of pyroprobe where the sample is contained in a removable quartz tube. In both cases, there is a fraction of the product gases that is not measured, namely higher hydrocarbon gases, such as C_2H_4, C_2H_6, C_3H_6 and C_3H_8 as well as H_2 in the case of the HF reactor and H_2O in the case of pyroprobe. The total yield of higher hydrocarbon gases can sum up to 2–5 wt% depending always on the experimental conditions and the biomass type [51,56,58], while the H_2 production is usually close to, or less than 1 wt%, as it was also shown in the present study [50,59]. For both cases however, the largest amount of losses can be attributed to the liquid product gravimetric measurements. As it was shown in Section 3.1, the HF reactor fails in terms of PAH determination by underestimating their total yield even by 5 times compared to the PP. However, the main drawback of the PP system is the inability to measure gravimetrically the products condensing in the impinger trap. As it was shown in Fig. 3, as temperature increases the bigger part of the PAH condenses there. Lighter tar compounds are also expected to be found present in significant quantities in the impinger trap rather than in the quartz trap. Furthermore, as it was also mentioned earlier, there is a possibility of heavy PAH condensation in the transfer tube situated in the oven area of the PP reactor. Finally, pyrolytic water production was not measured for the PP experiments, in contrast with the HF tests. Pyrolytic water can account for 10–12 wt% of the dry feed [60–62] and part of it condenses in the impinger trap for the PP experiments.

4. Conclusions

Fast pyrolysis of woody (softwood mixtures) biomass was conducted in a Pyroprobe (PP) reactor, with the purpose of studying PAH formation at high pyrolysis temperatures with an efficient, accurate and user – friendly method. Comparison of the results with the ones obtained from experiments conducted with a heated foil (HF) reactor showed a definite improvement in terms of PAH capture, with the exception of some heavier PAH, which however contribute very little to the overall PAH yield. The PP reactor was also more efficient with respect to the total yields determination, due to the absence of thermal lag at lower temperatures, that leads to higher char yields for reactors such as the HF. Overall, it was also concluded that the HF reactor is not applicable for PAH quantification related studies, without making significant changes in the reactor's configuration (sample size, pyrolysis chamber size, etc.) and tar sampling methods.

PAH yields were found to increase with increasing pyrolysis temperature approaching a maximum of 1900 mg/kg (roughly 0.2 wt% of the overall yield) at 1000 °C for the PP experiments. Naphthalene and acenapthylene were the main compounds detected, while also significant amounts of phenanthrene were detected. PAH evolution was linked with the simultaneous increase of the CO, H_2 and CH_4 yields, the stabilization of the char yield and the decrease of the liquid yield, suggesting that it is mainly a product of secondary decomposition.

The PP system produced reasonably good mass balance closure values (80 wt% on average). Char and gas yields were determined with high accuracy, however gravimetric liquid analysis lacked in this sense mainly due to the inability to measure the yield condensing in the impinger bottle. There is a trade – off between the gravimetric determination of the total liquid yield and the quantification of its constituents. By adding a solvent evaporation step for example, one might improve the mass balance closure values, but at the same time it would hamper the efficiency of determination of the liquid compounds. It was shown, that while a single cold trap is sufficient for PAH condensation at low concentrations (and therefore low pyrolysis temperatures), the same does not hold for higher concentrations. Therefore, an expanded condensation/trapping system, such as the one presented here, is required.

Overall, the proposed system was successful in the reproducible quantification of PAH produced from biomass fast pyrolysis experiments. The flexibility of the system allows the fast conduction of multiple experiments, which minimizes the time required for sampling and its complexity. Furthermore, specific compounds of interest can be targeted for the analysis (PAH, sugars, acids, phenolics, etc.), depending on the experimental conditions and the purpose of the study.

CRediT authorship contribution statement

C. Tsekos: Formal analysis, Writing - original draft, Writing - review & editing, Visualization. **K. Anastasakis:** Conceptualization, Methodology, Investigation, Validation, Visualization, Writing - review & editing. **P.L. Schoenmakers:** Investigation. **W. de Jong:** Writing - review & editing, Supervision, Project administration, Funding acquisition.

Declaration of Competing Interest

The authors declare that they have no known competing financial interests or personal relationships that could have appeared to influence the work reported in this paper.

Acknowledgements

The authors are grateful to the Groen Gas project of Rijksdienst voor Ondernemend Nederland (RvO) (reference no. TKIG01040) and to the European Biofuels Research Infrastructure for Sharing Knowledge (BRISK) project (contract no. 284498) for funding. The authors would also like to thank Synvalor for supplying of the biomass samples.

References

[1] S. Wang, et al., Lignocellulosic biomass pyrolysis mechanism: a state-of-the-art review, Prog. Energy Combust. Sci. 62 (2017) 33–86.
[2] P. Basu, Biomass Gasification and Pyrolysis Practical Design and Theory, Elsevier Inc., 2010.
[3] A. Dufour, et al., Evolution of aromatic tar composition in relation to methane and ethylene from biomass pyrolysis-gasification, Energy Fuels 25 (2011) 4182–4189.
[4] L. Devi, K.J. Ptasinski, F.J.J.G. Janssen, A review of the primary measures for tar elimination in biomass gasification processes, Biomass Bioenergy 24 (2) (2003) 125–140.
[5] P. Basu, Combustion and Gasification in Fluidized Beds, Taylor and Francis, 2006.
[6] C. Li, K. Suzuki, Tar property, analysis, reforming mechanism and model for biomass gasification—an overview, Renewable Sustainable Energy Rev. 13 (3) (2009) 594–604.
[7] H. Pakdel, C. Roy, Hydrocarbon content of liquid products and tar from pyrolysis and gasification of wood, Energy Fuels 5 (3) (1991) 427–436.
[8] S. Boonchan, M.L. Britz, G.A. Stanley, Degradation and mineralization of high-molecular-Weight polycyclic aromatic hydrocarbons by defined fungal-bacterial cocultures, Appl. Environ. Microbiol. 66 (3) (2000) 1007.
[9] T. McGrath, R. Sharma, M. Hajaligol, An experimental investigation into the formation of polycyclic-aromatic hydrocarbons (PAH) from pyrolysis of biomass materials, Fuel 80 (12) (2001) 1787–1797.
[10] T.A. Milne, R.J. Evans, N. Abatzoglou, Biomass Gasifier "Tars": Their Nature, Formation, and Conversion, National Renewable Energy Laboratory (NREL), 1998.
[11] L. Devi, et al., Catalytic decomposition of biomass tars: use of dolomite and untreated olivine, Renew. Energy 30 (4) (2005) 565–587.
[12] P.R. Solomon, M.A. Serio, E.M. Suuberg, Coal pyrolysis: experiments, kinetic rates and mechanisms, Prog. Energy Combust. Sci. 18 (2) (1992) 133–220.
[13] E. Jakab, et al., Chapter 3, A. Pandey (Ed.), Analytical Techniques as a Tool to Understand the Reaction Mechanism, in Recent Advances in Thermo-Chemical Conversion of Biomass, Elsevier, Boston, 2015, pp. 75–108.
[14] C. Tsekos, Fast Pyrolysis of Woody Biomass in a Pyroprobe Reactor: Effect of Torrefaction on the Pyrolysis Products, Delft University of Technology: Delft, 2016.
[15] G. Di Nola, Biomass Fuel Characterization for NOx Emissions in Cofiring

Applications, in Mechanical, Maritime and Materials Engineering, Delft University of Technology: Delft., 2007.
[16] A. Dufour, et al., Comparison of two methods of measuring wood pyrolysis tar, J. Chromatogr. A 1164 (1) (2007) 240–247.
[17] H. Zhou, et al., Effect of interactions of biomass constituents on polycyclic aromatic hydrocarbons (PAH) formation during fast pyrolysis, J. Anal. Appl. Pyrolysis 110 (2014) 264–269.
[18] H. Zhou, et al., Polycyclic aromatic hydrocarbon formation from the Pyrolysis/Gasification of lignin at different reaction conditions, Energy Fuels 28 (10) (2014) 6371–6379.
[19] Y. Zhang, et al., Tar destruction and coke formation during rapid pyrolysis and gasification of biomass in a drop-tube furnace, Fuel 89 (2) (2010) 302–309.
[20] Y. Zhang, et al., Peculiarities of rapid pyrolysis of biomass covering medium- and high-temperature ranges, Energy Fuels 20 (6) (2006) 2705–2712.
[21] N.E. Sánchez, et al., Formation of PAH and soot during acetylene pyrolysis at different gas residence times and reaction temperatures, Energy 43 (1) (2012) 30–36.
[22] D. Fabbri, A. Adamiano, C. Torri, GC-MS determination of polycyclic aromatic hydrocarbons evolved from pyrolysis of biomass, Anal. Bioanal. Chem. 397 (1) (2010) 309–317.
[23] J.A. Caballero, et al., Flash pyrolysis of Klason lignin in a Pyroprobe 1000, J. Anal. Appl. Pyrolysis 27 (2) (1993) 221–244.
[24] A.N. García, R. Font, A. Marcilla, Kinetic studies of the primary pyrolysis of municipal solid waste in a Pyroprobe 1000, J. Anal. Appl. Pyrolysis 23 (1) (1992) 99–119.
[25] R. Fahmi, et al., The effect of alkali metals on combustion and pyrolysis of Lolium and Festuca grasses, switchgrass and willow, Fuel 86 (10) (2007) 1560–1569.
[26] S. Kelkar, et al., Aromatics from biomass pyrolysis vapour using a bifunctional mesoporous catalyst, Green Chem. 16 (2) (2014) 803–812.
[27] S. Wang, et al., Mechanism research on cellulose pyrolysis by Py-GC/MS and subsequent density functional theory studies, Bioresour. Technol. 104 (2012) 722–728.
[28] A.B. Ross, et al., Investigation of the pyrolysis behaviour of brown algae before and after pre-treatment using PY-GC/MS and TGA, J. Anal. Appl. Pyrolysis 85 (1) (2009) 3–10.
[29] Q. Lu, et al., Influence of pyrolysis temperature and time on the cellulose fast pyrolysis products: analytical Py-GC/MS study, J. Anal. Appl. Pyrolysis 92 (2) (2011) 430–438.
[30] S. Zhang, et al., Effects of water washing and torrefaction on the pyrolysis behavior and kinetics of rice husk through TGA and Py-GC/MS, Bioresour. Technol. 199 (2016) 352–361.
[31] J. Zhao, et al., Thermal degradation of softwood lignin and hardwood lignin by TG-FTIR and Py-GC/MS, Polym. Degrad. Stab. 108 (2014) 133–138.
[32] C.M. White, Prediction of the boiling point, heat of vaporization, and vapor pressure at various temperatures for polycyclic aromatic hydrocarbons, J. Chem. Eng. Data 31 (1986) 198–203.
[33] M. Zhang, F.L.P. Resende, A. Moutsoglou, Catalytic fast pyrolysis of aspen lignin via Py-GC/MS, Fuel 116 (2014) 358–369.
[34] J.A. González-Pérez, et al., Appraisal of polycyclic aromatic hydrocarbons (PAHs) in environmental matrices by analytical pyrolysis (Py–GC/MS), J. Anal. Appl. Pyrolysis 109 (2014) 1–8.
[35] B. Zhang, et al., Production of aromatic hydrocarbons from catalytic co-pyrolysis of biomass and high density polyethylene: analytical Py–GC/MS study, Fuel 139 (2015) 622–628.
[36] K. Anastasakis, I. Kitsiou, W. de Jong, Fast devolatilization characteristics of 'low cost' biomass fuels, wood and reed. Potential feedstock for gasification, Fuel Process. Technol. 142 (2016) 157–166.
[37] K. Anastasakis, C. Saenz, W. de Jong, Modeling physical phenomena during fast pyrolysis of biomass in a heated foil reactor, 21st International Symposium on Analytical and Applied Pyrolysis, Nancy, 2016.
[38] United States Environmental Protection Agency (EPA), Method 610: Polynuclear Aromatic Hydrocarbons, [cited 2019 25/11/2019]; Available from: (1984) https://www.epa.gov/sites/production/files/2015-10/documents/method_610_1984.pdf.
[39] P. Oesch, E. Leppämäki, P. Ståhlberg, Sampling and characterization of high-molecular-weight polyaromatic tar compounds formed in the pressurized fluidized-bed gasification of biomass, Fuel 75 (12) (1996) 1406–1412.
[40] C.A. Jordan, G. Akay, Effect of CaO on tar production and dew point depression during gasification of fuel cane bagasse in a novel downdraft gasifier, Fuel Process. Technol. 106 (2013) 654–660.
[41] P. Morf, P. Hasler, T. Nussbaumer, Mechanisms and kinetics of homogeneous secondary reactions of tar from continuous pyrolysis of wood chips, Fuel 81 (7) (2002) 843–853.
[42] G.A. Tsalidis, et al., The impact of dry torrefaction on the fast pyrolysis behavior of ash wood and commercial Dutch mixed wood in a pyroprobe, Fuel Process. Technol. 177 (2018) 255–265.
[43] C. Brage, Q. Yu, K. Sjöström, Characteristics of evolution of tar from wood pyrolysis in a fixed-bed reactor, Fuel 75 (2) (1996) 213–219.
[44] R. Cypres, Aromatic hydrocarbons formation during coal pyrolysis, Fuel Process. Technol. 15 (1987) 1–15.
[45] H. Yu, et al., Characteristics of tar formation during cellulose, hemicellulose and lignin gasification, Fuel 118 (2014) 250–256.
[46] S. Vichaphund, et al., Production of aromatic compounds from catalytic fast pyrolysis of Jatropha residues using metal/HZSM-5 prepared by ion-exchange and impregnation methods, Renew. Energy 79 (2015) 28–37.
[47] L. Sun, et al., Comparision of catalytic fast pyrolysis of biomass to aromatic hydrocarbons over ZSM-5 and Fe/ZSM-5 catalysts, J. Anal. Appl. Pyrolysis 121 (2016) 342–346.
[48] A. Trubetskaya, N. Souihi, K. Umeki, Categorization of tars from fast pyrolysis of pure lignocellulosic compounds at high temperature, Renew. Energy 141 (2019) 751–759.
[49] P.A. Horne, P.T. Williams, Influence of temperature on the products from the flash pyrolysis of biomass, Fuel 75 (9) (1996) 1051–1059.
[50] R.M. Hajaligol Mohammed, Product compositions and kinetics for rapid pyrolysis of cellulose, Ind. Eng. Chem. Process. Des. Dev. 21 (3) (1982) 457.
[51] R.T. Nunn Theodore, Product compositions and kinetics in the rapid pyrolysis of sweet gum hardwood, Ind. Eng. Chem. Process. Des. Dev. 24 (3) (1985) 836.
[52] E. Hoekstra, et al., Fast pyrolysis in a novel wire-mesh reactor: decomposition of pine wood and model compounds, Chem. Eng. J. 187 (2012) 172–184.
[53] A. Dufour, et al., Synthesis gas production by biomass pyrolysis: effect of reactor temperature on product distribution, Int. J. Hydrogen Energy 34 (4) (2009) 1726–1734.
[54] J.L. Figueiredo, et al., Pyrolysis of holm-oak wood: influence of temperature and particle size, Fuel 68 (8) (1989) 1012–1016.
[55] J.A. Caballero, R. Font, A. Marcilla, Kinetic study of the secondary thermal decomposition of Kraft lignin, J. Anal. Appl. Pyrolysis 38 (1) (1996) 131–152.
[56] M. Becidan, Ø. Skreiberg, J.E. Hustad, Products distribution and gas release in pyrolysis of thermally thick biomass residues samples, J. Anal. Appl. Pyrolysis 78 (1) (2007) 207–213.
[57] M. Jahirul, et al., Biofuels production through biomass pyrolysis —a technological review, Energies 5 (12) (2012) 4952.
[58] A.V. Bridgwater, G.V.C. Peacocke, Fast pyrolysis processes for biomass, Renewable Sustainable Energy Rev. 4 (1) (2000) 1–73.
[59] C. Di Blasi, et al., Product distribution from pyrolysis of wood and agricultural residues, Ind. Eng. Chem. Res. 38 (6) (1999) 2216–2224.
[60] A.G. Liden, F. Berruti, D.S. Scott, A kinetic model for the production of liquids from the flash pyrolysis of biomass, Chem. Eng. Commun. 65 (1) (1988) 207–221.
[61] D. Mohan, C.U. Pittman, P.H. Steele, Pyrolysis of Wood/Biomass for bio-oil: a critical review, Energy Fuels 20 (3) (2006) 848–889.
[62] A.V. Bridgwater, D. Meier, D. Radlein, An overview of fast pyrolysis of biomass, Org. Geochem. 30 (12) (1999) 1479–1493.